Synthesis and Characterization of Amino acid Functionalized Gold Nanoparticles and their Interaction with Lipid Membrane

M.Sc. Thesis

by

Avijit Maity
1703131004

DISCIPLINE OF CHEMISTRY
INDIAN INSTITUTE OF TECHNOLOGY INDORE
JUNE 2019

Synthesis and Characterization of Amino acid Functionalized Gold Nanoparticles and their Interaction with lipid membrane

A THESIS

Submitted in partial fulfillment of the
requirements for the award of the degree
of
Master of Science

by
Avijit Maity

DISCIPLINE OF CHEMISTRY
INDIAN INSTITUTE OF TECHNOLOGY INDORE
JUNE 2019

INDIAN INSTITUTE OF TECHNOLOGY INDORE

CANDIDATE'S DECLARATION

I hereby certify that the work which is being presented in the thesis entitled **Synthesis and characterization of amino acid functionalized gold nanoparticles and their interaction with lipid membrane** in the partial fulfillment of the requirements for the award of the degree of **MASTER OF SCIENCE** and submitted in the **DISCIPLINE OF CHEMISTRY, Indian Institute of Technology Indore**, is an authentic record of my own work carried out during the time period from July 2018 to June 2019 under the supervision of Dr. Anjan Chakraborty, Associate Professor, IIT Indore.

The matter presented in this thesis has not been submitted by me for the award of any other degree of this or any other institute.

Avijit Maity

This is to certify that the above statement made by the candidate is correct to the best of my/our knowledge.

Dr. Anjan Chakraborty

Avijit Maity has successfully given his M.Sc. Oral Examination held on **1st July 2019.**

Signature of Supervisor of MSc thesis — Convener, DPGC

Date: — Date:

Signature of PSPC Member — Signature of PSPC Member

Date: — Date:

Signature of PSPC Member

Date:

ACKNOWLEDGMENTS

I would like to give my deepest gratitude to my supervisor, **Dr. Anjan Chakraborty** for his continuous guidance and support during this project work. I thank him not only providing lab facility but also for his motivation towards research and advice for future plan of life.

I will also like to thank Dr. Tridib Kumar Sarma and Dr. Satya. S. Bulusu and Dr. Apurba K Das for their help in various aspects.

I am also very much grateful to Mr. Soumya Kanti De for his valuable suggestion and continuous help towards every field of this project. I am also thankful to Ms. Nishu Kanwa for her helping hands and cooperation in this work.

Moreover, I am filled with gratitude to my family and friends for staying with me in my bad times.

Finally, I would like to thank Sophisticated Instrumentation Center (SIC), IIT Indore and IIT Indore for providing infrastructure to conduct my research project.

Avijit Maity

M.Sc. 2nd year

Dedicated to My Family

Abstract

Herein, we have synthesized different aromatic amino acid functionalized gold nanoparticles and studied their interaction with different lipid membranes. We used three aromatic amino acids, namely, Phenylalanine (Phe), Tryptophan (Trp), Tyrosine (Tyr) to synthesize the nanoparticles in an in situ method. The synthesized nanoparticles are of the size around 10-15 nm characterized by UV-Visible absorption spectra, Transmission Electron Microscopy (TEM) and Zeta potential Measurements. The modulation of the size of the nanoparticles can be done by varying the concentration of the amino acids. The nanoparticles are fairly stable in the pH range from 10 to 6.5, however, at lower pH, the aggregation takes place due to protonation of COO^- group. We find that the synthesized nanoparticles were fluorescent in nature and we confirm this by steady-state and time-resolved fluorescence spectroscopy. We studied the interaction of the nanoparticles with lipid membrane of different charges. It is observed that the amino acid functionalized nanoparticles bring in dehydration in the lipid bilayer by the expulsion of the surface water. The maximum interaction takes place in case of negatively charged lipid membrane while positively charged lipid membranes exhibit the least interaction with the nanoparticles and for tryptophan functionalized nanoparticles, aggregation is observed. The extent of the interaction of nanoparticles with lipid membranes is governed by the bulkiness of the ligand. We find that the phenylalanine functionalized nanoparticles display maximum interaction to the lipid membrane.

TABLE OF CONTENTS

LIST OF FIGURES

LIST OF TABLES

NOMENCLATURE

nm	Nanometer
nM	Nanomolar
°C	Degree centigrade
τ_i	Lifetime of the i^{th} component
χ^2	Reduced chi-square Amplitude of the i^{th} component
a_i	Amplitude of the i^{th} component in a multiexponential decay
keV	Kilo electron volt
D(t)	Normalized Fluorescence Decay

ACRONYMS

AuNP	Gold Nanoparticle
Phe	Phenylalanine
Tyr	Tyrosine
Trp	Tryptophan
MLV	Multi-Lamellar Vesicle
LUV	Large Unilamellar Vesicle
GUV	Giant Unilamellar Vesicle
SUV	Small Unilamellar Vesicle
DMPC	1,2-dimyristoyl-sn-glycero-3-Phosphocholine
DMPG	1,2-dimyristoyl-sn-glycero-3-phospho-(1'-rac-glycerol)
DOTAP	1,2-dioleoyl-3-trimethylammonium-propane
PRODAN	6-Propionyl-2-Dimethylaminonaphthalene
$HAuCl_4$	Tetrachloroauric(III) acid
NaOH	Sodium Hydroxide
TEM	Transmission Electron Microscopy
AA	Amino Acid
TCSPC	Time-Correlated Single Photon Counting
MPA	3-mercaptopropanic acid
SPR	Surface Plasmon Resonance

Chapter 1

Introduction

(1.1) Gold Nanoparticles: Gold nanoparticles are an emerging area of interest these days considering their wide variety of applications in nanotechnology, biology and catalysis because of their size-dependent optical, magnetic and electric properties [1-6]. They also display some unique surface properties which are quite unlike those of other metal atoms as well as a bulk matter [7-12]. Gold nanoparticles are synthesized in several ways, but the most convenient path for synthesis is the chemical reduction method which requires gold salt, reducing agent, solvent and stabilizing agent [13-16]. In this method, first gold salt dissolves in the solvent and then reducing agent is mixed to reduce the metal. However, the reduced metal is not stable which calls for the need of a stabilizing agent to stabilize the metal in that oxidation state. Sometimes reducing agents like citrate, amino acids, the block copolymer may act as both reducing as well as stabilizing agent [17-23]. Otherwise stabilizing agents like polymers or thiol ligands are added to form stable gold nanoparticles [24-26].

(1.2) Amino acid functionalized gold nanoparticles: Generally, gold salts are reduced by borohydride/citrate followed by some organic molecule that contains SH or NH_2 group as a capping agent or otherwise in the presence of capping agent gold salts are reduced to synthesize gold nanoparticles [27-28]. But during this ligand exchange or centrifugation to remove the by-products particle, gold nanoparticles can undergo aggregation which is one of the vital problems of the above method. So it is now very much necessary to prepare the gold nanoparticles in-situ in which reducing agents act as both reducing and stabilizing agent. It will diminish the chance of aggregation of the particle. Many researchers are looking forward to in-situ reductions by amine functionalized molecules; higher temperature is required for in-situ reductions [30-31]. Thus in-situ preparation of gold nanoparticles with ambient temperature is very helpful in biological systems.

Aromatic amino acids such as phenylalanine, tryptophan and tyrosine can be used to prepare the gold nanoparticles in-situ due to the presence of amine group in all three amino acids which act as both reducing and stabilizing agents. It is well reported that tryptophan and tyrosine can be used in electron/hydrogen transport via radical intermediates in biological systems [32-38]. So different types of ligands functionalized gold nanoparticles are prepared by using three different amino acid (phenylalanine, tryptophan, and tyrosine), gold salt and sodium hydroxide. First, we optimize the reaction condition by varying the concentration of gold salt, amino acid, sodium hydroxide to synthesize small size gold nanoparticles. There are very few reports in the literature that shows that these (tyrosine and tryptophan) amino acid-based peptides show fluorescence emission spectra which may be due to the oxidative derivatives of amino acids [39]. So fluorescence emission spectra of these three nanoparticles are to be studied in detail. Although peptide functionalized fluorescence gold nanoparticles have been synthesis successfully, these nanoparticles show unstable fluorescence properties [19, 39]. Surprisingly, we found simple aromatic amino acid functionalized gold nanoparticles can exhibit a stable wavelength-dependent photoluminescence property even after 3 months. The fluorescence properties of proteins are typically dominated by tryptophan along with minor fluorescence from tyrosine and phenylalanine. We found that among these nanoparticles Au-Tyro shows impressive photoluminescence than other nanoparticles.

(1.3) Lipid Bilayers(Liposomes): The composition of a cell membrane is mainly phospholipid and membrane proteins [40]. The lipid bilayer is very important because different structural compounds impact the barrier that surrounds the boundaries of a cell [41]. Lipids are composed of two important parts which form the lipid bilayer. The first part is the hydrophilic part which is also known as the polar head group and the other is the hydrophobic part which consists of the long hydrocarbon chain, known as the nonpolar tail. When the lipid molecules are injected in polar solvents like water they arrange themselves to form a lipid bilayer. Due to the formation of lipid bilayer hydrophilic parts

expose to polar solvents while hydrophobic parts hide their face from water molecules [41].

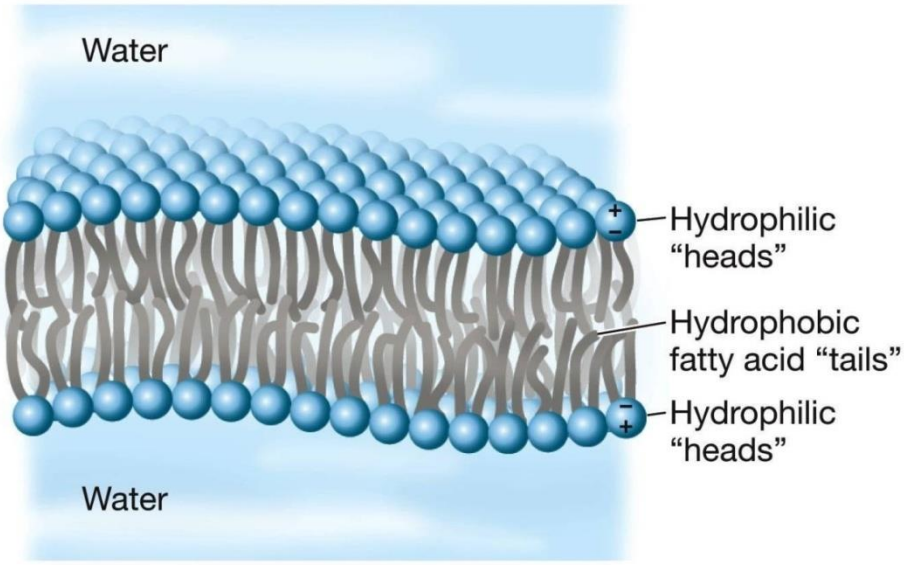

Figure 1: Phospholipid bilayer [42]

The phospholipids form the lipid bilayer through binding at the long hydrocarbon chain group of each other. Therefore the liposome which is formed from phospholipid is called the PC liposomes. In recent past, lipid bilayer membranes have drawn our attention to their interaction with metal ions, amino acids, polymer, nanoparticles [43-50]. Lipid bilayers are prepared from lipid by several methods (i) thin film hydration [51] (ii) reverse phase evaporation [52] (iii) solvent injection [53]. In terms of their size lipid bilayers can be classified as MLV- Multi-Lamellar Vesicle (>0.5µm), GUV- Giant Unilamellar Vesicle (>1µm), LUV- Large Unilamellar Vesicle (> 100 nm), SUV- Small Unilamellar Vesicle (20-100 nm).

Three differently surface charged lipids are commercially available. DMPC (1,2-dimyristoyl-sn-glycero-3- phosphocholine) is zwitterionic lipid molecule in which phosphate and choline groups are present i.e zwitterionic lipid, DMPG (1,2-

dimyristoyl-sn-glycero-3-phospho-(1'-rac-glycerol) (sodium salt) is negatively charged lipid in which only phosphate groups are present, DOTAP(1,2-dioleoyl-3-trimethylammonium-propane (chloride salt) is positively charged lipid in which only choline groups are present. **Figure 2** shows the structure of the three lipids.

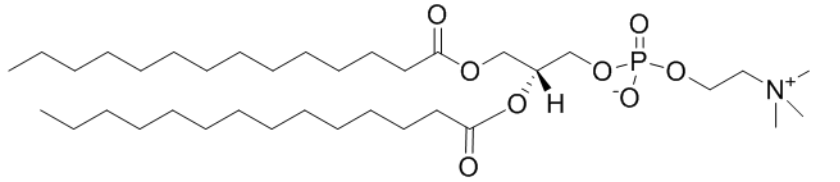

DMPC

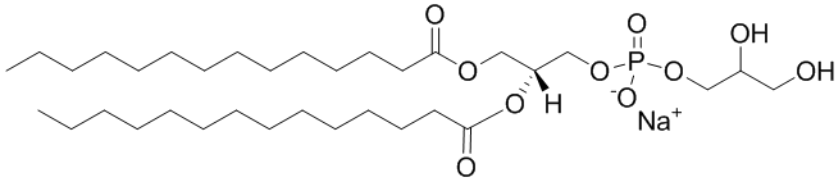

DMPG

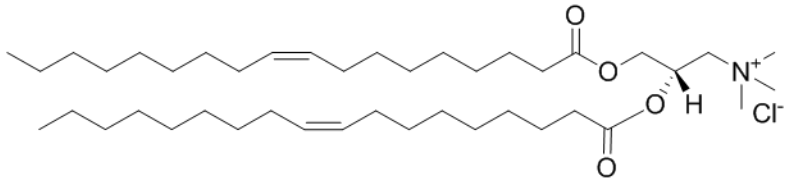

DOTAP

:

Figure 2: Molecular structure of the lipids (DMPC, DMPG, DOTAP).

(1.4) Studying the interaction of nanoparticles with lipid membrane: The interaction of metal nanoparticles and lipid bilayer is an exploring field as they usually give biocompatible systems [54-59]. Interaction of metal nanoparticles with three different surfaces charged lipid are very few in literature. Some of the nanoparticles dehydrate the bilayer [57]. The interaction between inorganic nanoparticle and lipid bilayer has been well reported in the

literature [60-63]. The Phosphate group in the lipid head group is responsible for the interaction of metal oxide nanoparticles with lipid bilayer [64-66].

Interaction of nanoparticles with zwitterionic lipid bilayer is very well known. Gold nanoparticles are of great interest among different types of nanoparticles. The surface morphology of gold nanoparticles can be easily changed by introducing different capping agents [17, 25]. Surface Plasmon coupling is responsible for gold nanoparticles to display distance dependent color [67-68]. When the surface of the lipid bilayer is coated with adsorbed high charged density nanoparticles, they stay more intact even 25% of the surface is covered [69]. So Interaction of different surface charged and different size ligand capped gold nanoparticles with different surface charged lipid bilayer will be very interesting. Hence we have taken three different aromatic amino acids which are different in size to synthesize the gold nanoparticles. Then we have studied the interaction of these nanoparticles with different surface charged lipid bilayer.

(1.5) Fluorescent Probes: Even though numerous studies on the interaction of lipid bilayer and gold nanoparticles have been explored, the literature demands more studies based on the spectroscope. For this context, fluorescence molecular probes can be used to study the changes in the fluorescence parameter of the bilayer membrane. Membrane polarity sensitive fluorescence probes are thus taken for this purpose. The emission wavelength, intensity can be monitored by using the fluorescence probe. PRODAN (6-Propionyl-2-Dimethylaminonaphthalene) and ANS (8-anilino-1- naphthalenesulphonate) are particularly used because these two are sensitive to the polarity of the surrounding medium [70-79]. **Figure 3** shows the structure of the PRODAN and ANS. In aqueous media, these two probe shows less intensity fluorescence but in membrane medium, they show large intensity fluorescence which is well studied in the literature [70-79]. When the solvent polarity is increased a large amount of redshift in the PRODAN emission spectra is noticed due to the dipolar relaxation phenomenon [71-72]. Charge transfer state for ANS in a polar medium is responsible for the quenching of fluorescence because it occurs via an electron

transfer process. The intense fluorescence for ANS in the hydrophobic environment is observed because the phenylamino group of ANS is restricted for rotational motion [70].

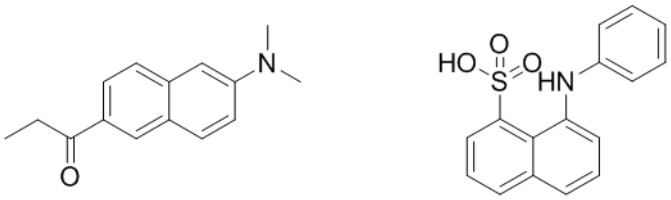

Figure 3: Molecular structure of PRODAN and ANS.

Chapter2

EXPERIMENTAL SECTION

(2.1) Chemicals and Reagents: All the three lipids DMPC (1,2-dimyristoyl-sn-glycero-3-phosphocholine) , DMPG (1,2-dimyristoyl-sn-glycero-3-phospho-(1'-rac-glycerol) (sodium salt), DOTAP (1,2-dioleoyl-3-trimethylammonium-propane(chloride salt) were purchased from Sigma-Aldrich. Chloroauric acid (HAuCl4.3H2O), Phenyl Alanine, Tryptophan, Tyrosine, PRODAN, ANS, HEPES were also purchased from Sigma-Aldrich whereas Sodium Hydroxide(NaOH) was purchased from Merck. We use all these chemicals as received. Milli-Q water was used to prepare all the solutions.

(2.2) Synthesis of amino acid functionalized Gold nanoparticles: Gold nanoparticles (Au NPs) were prepared by reducing gold ions using amino acids as reported earlier with slight modifications. Amino acids mediated synthesis of Au NPs was carried out at 80 C while varying the concentration of the precursors. To optimize the reaction condition, different concentration of aqueous metal ion (1×10^{-4} to 7.5×10^{-4} M) solution was added to different concentrations of amino acids (0.5×10^{-3} to 5×10^{-3} M). Briefly, 0.25 mL of required concentration of Chloroauric acid was added to 3.75 mL of Mili-Q water and the solution was heated up to 80 C. Then required concentration of 1 mL amino acid and followed by NaOH was added in the previous solution under the vigorous stirring condition for 1 hour. The changes were found in the color of the solution, which was from colorless to pink for the formation of AuNPs.To remove the unreacted metal ions and amino acids we dialysis the gold nanoparticle solution by a polycarbonate membrane (M.W cut off 12000 kD).

(2.3) Preparation of three Gold Nanoparticles with the optimized condition: All these three AuNPs were prepared by using three Amino acids namely Phenyl Alanine, Tryptophan, Tyrosine in the same procedure. 0.25 ml of Chloroauric solution (0.75 mM) was added in 3.75 ml of Mill Q and then the

solution was heated at 80 C. After a few minutes, 1ml of 1mM Amino acid solution was added in boiling $HAuCl_4$ solution followed by 20 mM NaOH. The resultant solution was kept under vigorous stirring for 1 hour until the ruby red solution was observed from a colorless solution. After 1 hour, the solution was kept at room temperature and then stored at 4 °C for further use.

(2.4) Fluorescence spectrum of Nanoparticles: To study the fluorescence emission and excitation spectrum of these three amino acids functionalized gold nanoparticles we diluted 10 times of the stock solution. Then we excited all these three nanoparticles in the range 280nm to 400nm and emission spectrum recorded. Similarly, we excited all these blank amino acids with the same concentration in the range 280 nm to 400 nm.

(2.5) Preparation of PRODAN solution: A stock solution of PRODAN was prepared in methanol. Then the required amount of stock solution of PRODAN was taken in a volumetric flask and dried under vacuum for a few minutes. An appropriate amount of Milli Q was then added to the volumetric flask to obtain a 2 µM PRODAN solution.

(2.6) Preparation of Lipid Vesicles: Lipid vesicles were prepared in HEPES buffer solution (pH=7.0). First PRODAN solution was heated above the phase transition temperature of a particular lipid. Then the specific lipid was dissolved in ethanol (0.01% of the hydrating solution) and injected in the preheated PRODAN solution. After 1 hour stirring of the solution heating was stopped and also cooled for an hour before performing any studies. The lipid concentration was fixed at 0.1mM while the PRODAN concentration ware fixed 2µM.

(2.7) Instrumentation: Varian UV-vis spectrophotometer (Cary 100 Bio) in a quartz cuvette (10 × 10 mm2) was used to record the absorption spectra of AuNPs. The morphology of the synthesized amino acid functionalized gold nanoparticles were studied by Transmission Electron Microscope(TEM), was

conducted using a Tecnai T20 transmission electron microscope with an operating voltage of 200 keV. ζ potential of the synthesized AuNps was measured using NanoPlus ζ/particle size analyzer (NanoPlus-3 model). FluoroMax-4p spectrofluorometer from Horiba Jobin Yvon (model: FM100) was used to record the steady-state fluorescence spectra. OriginPro 8.1 software was also used to analyze all the emission spectra. We varied the gold nanoparticles concentration (0-10 nM) while the lipid (0.1mM) and PRODAN (2μM) concentration remain fixed to investigate the interaction of lipid vesicle and different Amino acid functionalized gold nanoparticles. All the samples were excited at 375nm. We use 2/2 nm slit for excitation and emission spectra for all emission spectra of PRODAN. The temperature (25 °C), pH (7.0), were always kept constant throughout all measurements. Picosecond TCSPC machine from Horiba (FluoroCube- 01-NL) was used for lifetime measurements. Here we excited the samples at 375nm using a picosecond diode laser (model: Pico Brite-375L) and collected decays of the sample at 440nm and 490 nm. A filter on the emission side was also placed to eliminate the scattered light. The signals were collected at a magic angle (54.75°) polarization using a photomultiplier tube (TBX-07C) as the detector. The full width at half-maximum of the instrument response function of our setup was ~140 ps. The data analysis was performed using IBH DAS version 6 decay analysis software. We fixed the temperature at 25 C throughout all titration experiments. The decays were fitted with a multiexponential function.

$$D(t) = \sum_{i=1}^{n} a_i \exp\left(\frac{-t}{\tau_i}\right)$$

where D(t) denotes normalized fluorescence decay and a_i is the normalized amplitude of decay component τi. The average lifetime was obtained from the equation

$$\langle\tau\rangle = \sum_{i=1}^{n} a_i \tau_i$$

The quality of fit was judged by reduced χ2 values and corresponding residual distribution. The acceptable fit has a χ2 near unity.

Chapter 3

RESULTS AND DISCUSSION

(3.1) Optimization and Characterization of differently functionalized AuNPs:

Herein, we synthesized three different amino acid capped gold nanoparticles by using three aromatic amino acids namely a) Phenylalanine b) Tryptophan c) Tyrosine [80-82]. **Figure 4 (a-c)** shows the structure of the three amino acids.

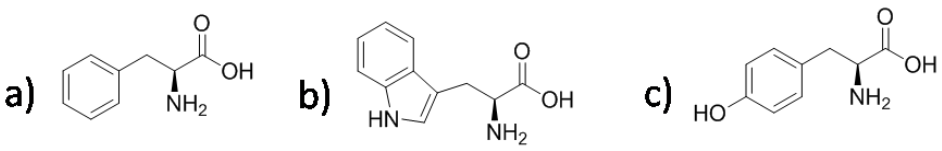

Figure 4: Molecular structure of **a)** Phenylalanine **b)** Tryptophan **c)** Tyrosine.

As mentioned in the materials and methods section, the reaction was demonstrated by addition of 1.0×10^{-4} M to 7.5×10^{-4} M of $HAuCl_4$ ions to various concentrations of amino acids ranging from 0.5×10^{-3} M to 5×10^{-3} M in aqueous medium under 80°C and vigorous stirring. The colorless solution gradually changed to intense pink during the formation of Au-AA NPs depending on the concentration of amino acids used in the reaction mixture. The reaction was completed within 1 hour, and no further change in the color was noted, indicating the formation of Au-AA NPs, where amino acids act as a reducing as well as a stabilizing agent. The formation of Au-AA NPs was confirmed by the appearance of surface plasmon resonance (SPR) peak from UV−visible spectra. Effect of Au^{3+}, NaOH and amino acids concentration on the formation of Au-AA NPs were summarized in **figure 5 (a-i)**. Sharp SPR peak at ~520 nm was observed for amino acids capped Au NPs when the concentration of $HAuCl_4$, amino acids, and sodium hydroxide was 7.5×10^{-4} M, 1×10^{-3} M and 20 mM respectively, as shown in **figure 7 (a). Figure 6** gives one important observation is that Tyr and Phe are unable to form NPs in absence of NaOH but Trp residue results in an instantaneous formation of NPs with slight broadness in SPR peak. Which lead us to conclude that the secondary amine group in the indole ring in

Tryptophan can also reduce the $Au^{3+}$to Au NPs.We also found that excess NaOH or the addition of NaOH prior to amino acids in the $HAuCl_4$ solution prevents the formation of Au NPs by forming $Au(OH)_3$.

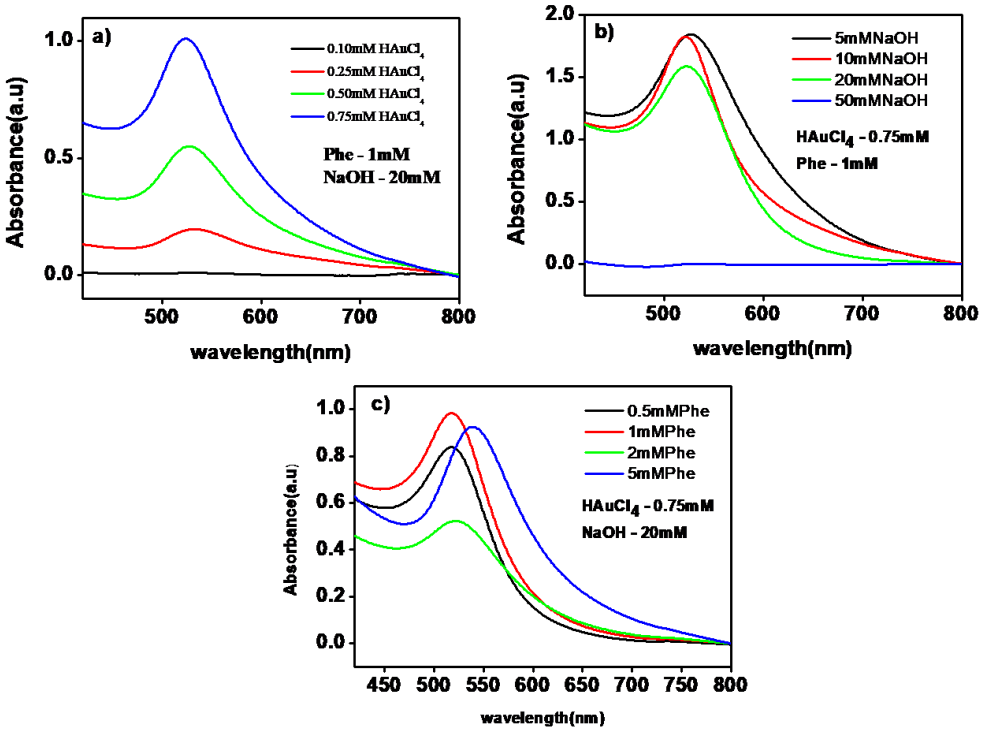

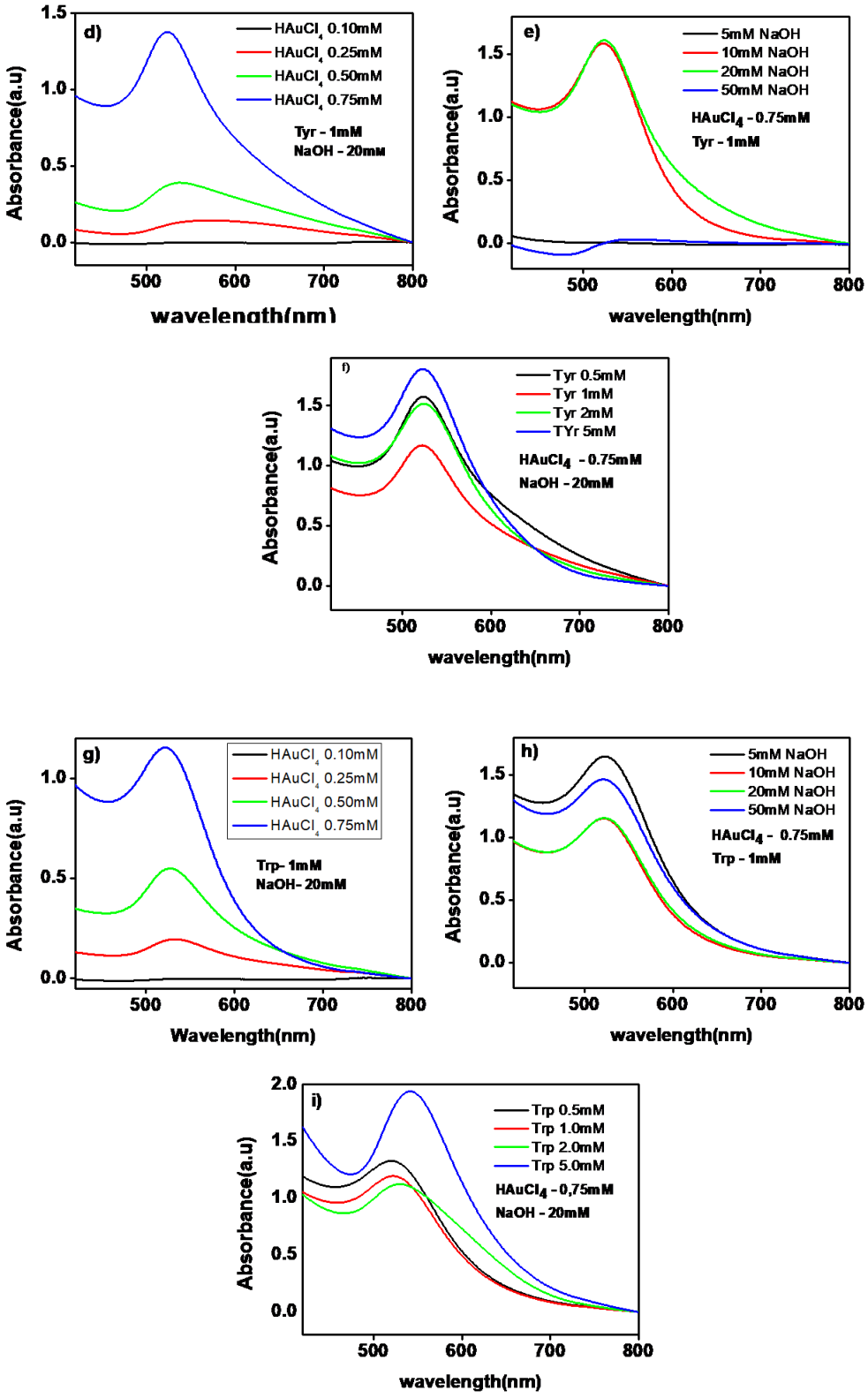

Figure 5: UV-Visible absorption spectrum of AuNPs at various concentration of Au^{3+}, amino acid and NaOH **(a-i).**

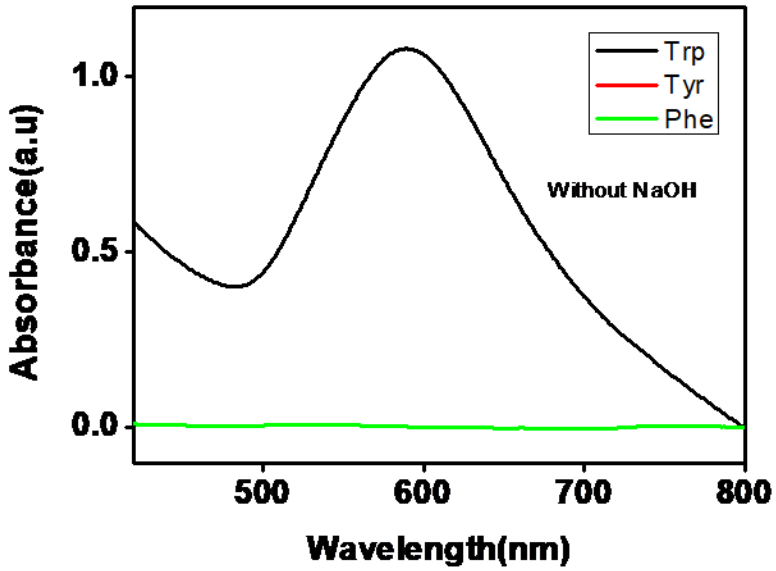

Figure 6: UV-visible spectrum of AuNPs without adding NaOH.

With increasing concentration of amino acids broadening of the SPR peak of the gold nanoparticle was found which indicates the formation of larger size Au-AA NPs in the case of Phe and Trp. Interestingly, we did not observe the broadening of the SPR peak of Au-Tyr NPs even in the presence of a high concentration of Tyrosine. We believe that the intramolecular hydrogen bonding of Tyr plays a crucial role in such deviation. Tyr is less soluble in water than Phe and Tyr because of its intramolecular hydrogen bonding. We assume that the nucleation process involves a fixed number of Tyr molecule and at high concentration excess Tyr did not involve in the nucleation process and did not affect the size (or SPR peak) of the AuNPs. Figure **7 (c)** demonstrate the zeta potential of the phenylalanine, tyrosine and tryptophan functionalized Au-AA NPs were found -34mV, -37mV and -32mV respectively in experimental pH (i,e pH~ 10).So, inhibition of nanoparticle formation in absence of NaOH and negatively charged zeta potential leads us to conclude that the amine group forms a covalent bond with AuNPs, and the deprotonated state of carboxyl group inhibits the aggregation of NPs by electrostatic repulsions between the NPs surface. Aggregations of NPs are effectively depending on the pH of the medium and water-dispersible NPs even in physiological pH have important implications in the biological context.

To evaluate the pH-dependent stability of colloidal nanoparticle solution we change the pH of the solution by the addition of HCl. Upon the addition of HCl to the Au-AA NPs solution from basic pH to neutral pH, we found a marginal shift of the SPR peak for all of these AuNPs in **figure 7(a) and 7(b).** The surface charge of these corresponding NPs also found to negative which indicates that Au-AA NPs are very stable in neutral to basic pH range. TEM images of the Au-Phe, Au-Tyr, and Au-Trp were shown in **Figure 7(d-f)**. The average diameter of the Au-AA NPs was found 16.0±0.7 nm (Au-Phe), 17.6±1.2 nm (Au-Tyr) and 7.9±0.3 nm (Au-Trp) from TEM measurements.

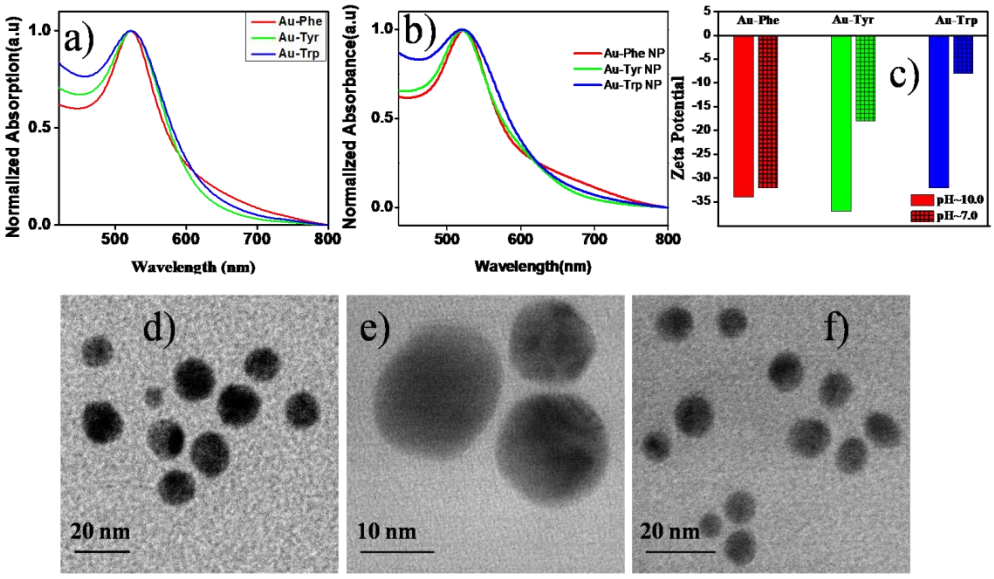

Figure 7: (a) UV-Visible spectrum of AuNPs at pH=9, **(b**) Zeta potential of AuNPs at pH=9 and pH=7, **(c-e)** TEM images of AuNPs at pH=9.

(3.2) Fluorescence Emission and Excitation spectra of AuNPs:

Surprisingly, excitation wavelength-dependent photoluminescence properties of aromatic amino acid functionalized Au NPs were observed in **figure 8(a-c)**. Maximum emission of the Au-Phe found at 425 nm upon excitation at 370 nm, whereas upon excitation at 320 nm, maximum emission intensity was found at 395 nm and 408 nm for Au-Trp and Au-Tyr respectively. The fluorescence of these aromatic amino acids is well reported in the literature. Phenylalanine and

tyrosine show an emission around ~300 nm whereas tryptophan shows emission maxima at 350 nm at water medium and tryptophan is much more fluorescent than either tyrosine or phenylalanine. So, it is very clear that the fluorescence properties of Au-AA NPs were very different from the blank amino acids. Further upon excitation at 310 nm none of this amino acid show any fluorescence spectra at the same concentration level present at Au-AA NPs solution, which confirms that individual fluorescence of blank amino acids does not responsible for the photoluminescence property of the Au-AA NPs. Excitation spectra of the corresponding fluorescence emission spectra of blank amino acids and Au-AA NPs were collected. The excitation spectra of the Phe, Tyr, and Trp were found 268 nm, 275 nm, and 273 nm respectively whereas, the spectra were red shifted in the case of all three Au-AA NPs. The excitation spectra of these Au-AA NPs were summarized in **Table 1**. The red-shifted excitation spectra indicate that the amino acids have a tendency to get aggregation in the surface of the gold nanoparticles. The fluorescence emission and excitation spectra of aromatic amino acids functionalized AuNPs and blank amino acids are shown in **figure 8 (d-f).**

Table1: Excitation-emission wavelength of the amino acids and amino acid stabilized Au NPs.

	Excitation (nm)	**Emission (nm)**		**Excitation (nm)**	**Emission (nm)**
Phe	268	302	Au-Phe	298 & 371	425
Tyr	274	298	Au-Tyr	314	407
Trp	273	348	Au-Trp	279 & 320	395

Tyrosine functionalized Au NPs show a complete shift of its excitation spectra to 314 nm from 274 nm corresponding to blank tyrosine. On the other hand,

tryptophan functionalized Au NPs show a new excitation peak at 320 nm along with the peak corresponding to blank tryptophan (~ 273 nm). Synthesis of Au NPs by tyrosine and tryptophan-containing oligopeptides at the C-terminus were previously reported. Mandal et al [19,39] reported that the tyrosine/tryptophan residue of the peptide donates an electron to the metal ion and is itself converted to a transient tyrosyl/tryptophyl radical, which eventually transforms to the highly fluorescent dityrosine/ditryptophan form of the peptide. Eventually, we also found that the Tyrosine functionalized Au NPs are highly fluorescent than Tryptophan functionalized Au NPs which is opposite fluorescence property of the blank amino acids. This observation can be explained from the complete shift of the excitation spectra at 314 nm of the Au-Tyr from blank tyrosine whereas the generation of a low-intensity new peak at 320 nm in case of tryptophan. We hypothesize that the tyrosine molecules are forming a complete conjugated structure (maybe di or poly tyrosine) due to the greater stability of tyrosyl radicals whereas fewer part of the tryptophan with less stable tryptophyl radical forming a di/poly tryptophan along with bare tryptophan. The greater conjugation of tyrosine than tryptophan is responsible for better fluorescence of Au-Tyr than Au-Trp NPs. Interestingly, a marginal peak shift (~100 nm) of the excitation spectra is observed in the case of Au-Phe. Unlike tyrosine and tryptophan, Phenylalanine does not have the opportunity to form a polymeric or dimeric form via radical formation. We hypothesize that Phe forms an aggregated structure between themselves without forming any bond via pia-pia stacking. The lifetime data of the AuNPs are shown in **figure 8 (g-i).**

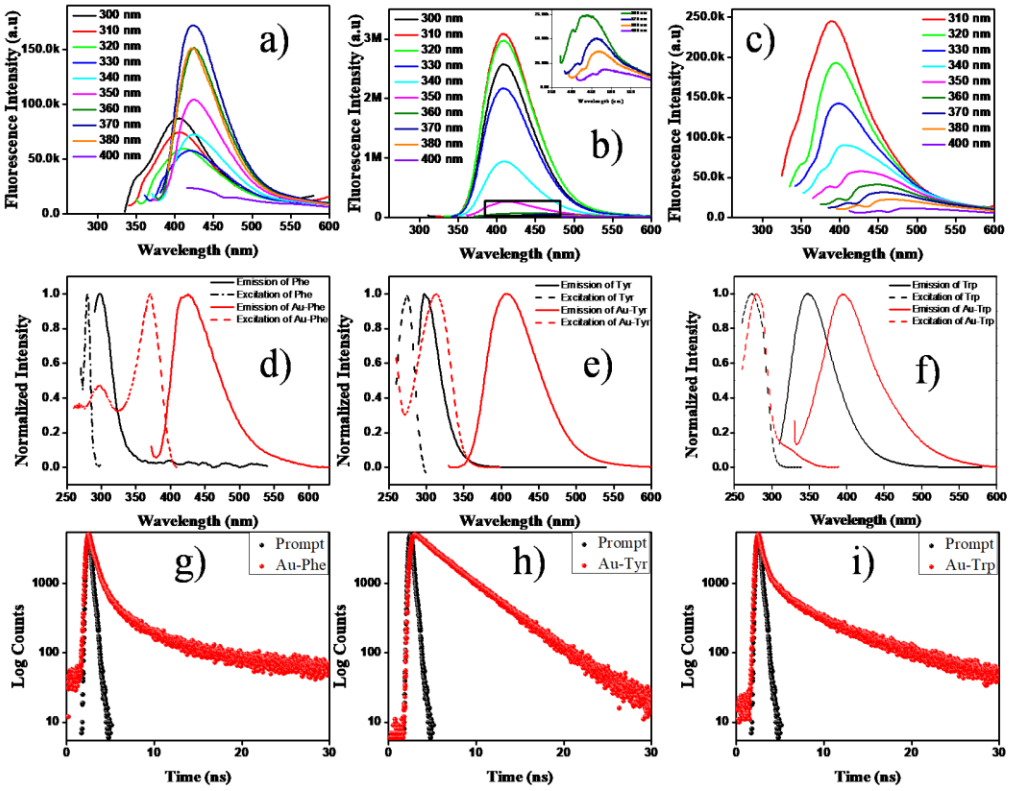

Figure 8: Excitation-wavelength-dependent PL spectra of **(a)** Au-Phe NPs; **(b)** Au-Tyr NPs; and **(c)** Au-Trp NPs. Excitation and emission spectra of the amino acids and amino acid stabilized Au NPs at maximum emission wavelength for **(d)** Phe; **(e)** Tyr; and **(f)** Trp. **(g-i)** TCSPC spectra of the resultant Au-AA NPs (λ_{ex} = 330 nm; λ_{em} = maximum emission wavelength, 25°C).

To evaluate our hypothesis and to detect the properties of the oxidation product of amino acids on the AuNPs surface, we exchange the Au NPs surface by a better ligand. We chose 3-mercaptopropanoic acid (MPA), which was added in excess to the Au-AA NPs and stirred for 24 hours. The interaction between -SH and Au surface is much stronger which replaces the weaker –NH/-NH_2 of an oxidation product of amino acids from the gold surface. After exchange by MPA, the mixture was centrifuged to separate the MPA-capped Au NPs, and the supernatant containing the oxidation product of amino acids were collected for fluorescence measurement. **Figure 9(b-d)** shows that the emission spectra from the supernatant appear in the same wavelength as for Au NPs solution. These results suggest that

the fluorescence from the Au-AA NPs completely driven by the oxidation product of the amino acids. The excitation spectra of the supernatant from Au-Tyr and Au-Trp remain unchanged as for AuNPs, i.e., the aggregation of tyrosine and tryptophan is irreversible which suggest the formation of di/poly amino acids. Interestingly the excitation spectra of the supernatant from Au-Phe were partly blue shifted corresponding to the peak for blank Phenylalanine. Summarized of these results suggest that the tyrosine and tryptophan forming a di/poly amino acid via free radical formation whereas phenylalanine forming an aggregation via pi-pi stacking on the surface of Au NPs.

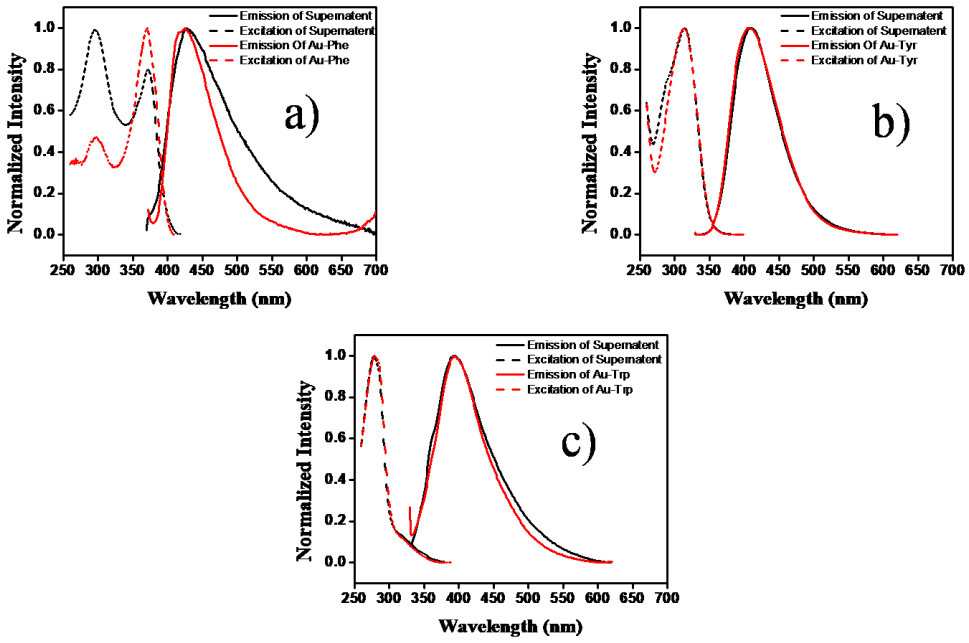

Figure 9: Comparison in fluorescence emission and excitation spectra of amino acid functionalized AuNPs and the supernatant solutions of the AuNPs after replacing by MPA**. a)** Au-Phe NP **(b)** Au-Tyr NP **c)** Au-Trp NP.

(3.3) Studying the interaction of AuNPs with lipid vesicles using PRODAN:

PRODAN exhibits high sensitivity towards solvent polarity. PRODAN has been very useful for studies of model membranes due to its high recognition of the different phase state of the membrane. In aqueous medium, it shows emission spectra at 520nm which is due to the internal charge-transfer state (ICT). In some reports, this state has been assigned as a twisted internal charge transfer state (TICT). However, in a lipid bilayer, it exhibits two emission peaks. One emission peak is at 490 nm due to the TICT state and another emission peak is at the 440nm due to the locally excited (LE) state. This emission spectra designate that PRODAN is partitioned in the lipid bilayer. Here we have taken three differently charged lipid- a) zwitterionic lipid (DMPC) b) positively charged lipid (DOTAP) c) negatively charged lipid (DMPG) to study the interactions with different AA functionalized gold nanoparticles.

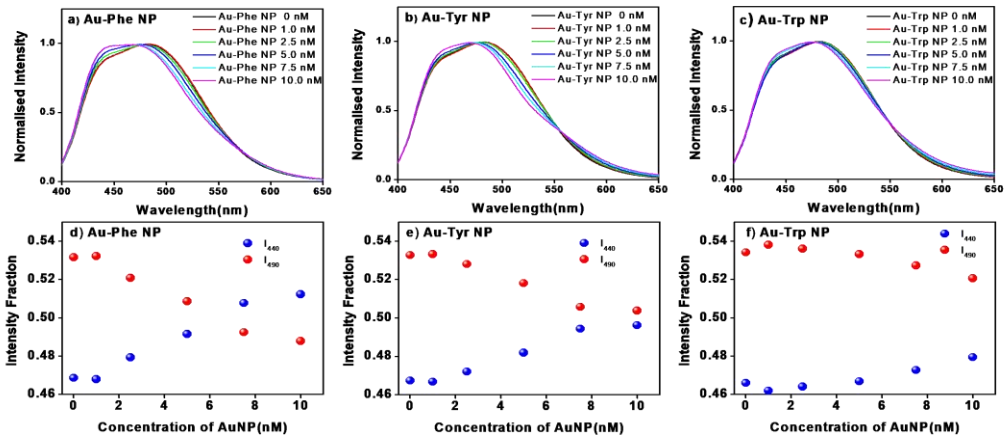

Figure 10: Steady-state normalized fluorescence spectra and corresponding area fraction plots for DMPC-PRODAN upon interaction with three AuNPs **(a-f)** at pH=7.

Initially, we study the interaction of different AA functionalized gold nanoparticles with zwitterionic lipid bilayer at pH 7. **Figure 10(a-e)** showed that the emission spectra of PRODAN is shifted to the lower wavelength due to the interaction of these three anionic gold nanoparticles with DMPC. The intensity

fraction plot also shows that the band corresponding to the LE state of PRODAN increases with the increase of the concentration of all these three AuNPs. The observed blue shift in the emission spectra indicates the dehydration of the lipid bilayer. The lipid undergoes a fluid-to-gel phase (Lα to Lβ) transition due to the adsorption of nanoparticles on the bilayer surface. This transition, however, takes place locally at the point of contact of the nanoparticles. Initially, the head group of the zwitterionic lipid is roughly parallel to the bilayer surface. However, upon addition of the nanoparticles, the head group tends to tilt so as to favor the interactions with the negatively charged AuNPs via the positively charged choline group. The maximum blue shift was observed for phenylalanine functionalized AuNP, followed by tyrosine and tryptophan functionalized AuNP. This observation is also clarified from the relative plot and generalized polarization plot of the intensity fraction in **Figure 11(a-b).**

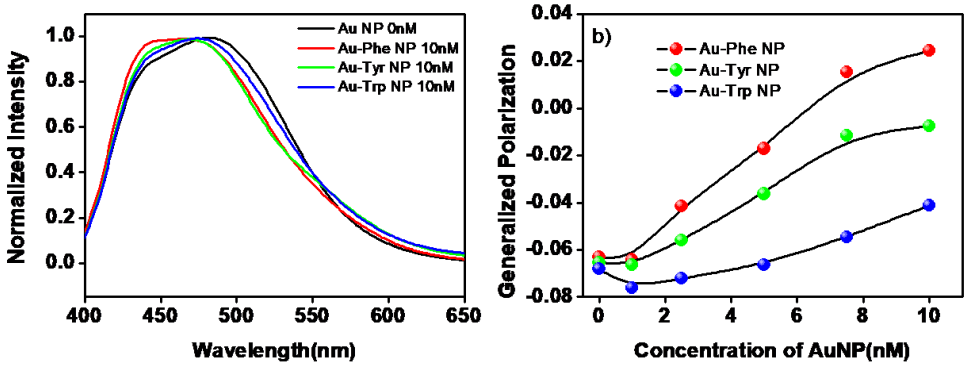

Figure 11: (a) Relative steady-state normalized fluorescence spectra of DMPC-PRODAN upon interaction with three AuNPs **(b)** Generalized Polarization data of the three AuNPs upon interaction with DMPC bilayer.

These data reveal that the lipid bilayer is more dehydrated upon interaction with Phenylalanine functionalized gold nanoparticle than the other two AuNPs. It is reported that chemisorption does not take place in the present case as a chemical reaction does not take place between lipid head groups and ligands or nanoparticles. The AuNPs undergo physisorption on the surface of the lipid vesicles that exert a strong van der Waals force. The interaction decreases with the increase of the bulkiness of the ligands, exerting lesser Van der Waals force.

The core distance of the AuNP from the bilayer phosphate group depends on the bulkiness of the ligands. Adsorption strength of any surface ligand depends on the small separation from the AuNP core. So the phenylalanine functionalized AuNP affect the packing of the bilayer which brings to a stronger gel phase. The bulkiness of the ligands follows the order: Phenylalanine> Tyrosine>Tryptophan. So the effectiveness of the ligand for lipid bilayer dehydration also follows the same order. Interestingly, **Figure 12(a-f)** revealed that the interaction of the AuNPs with lipid bilayer at pH=7 is stronger than that of pH=9. This may be due to the fact that at pH=7, the NH_2 groups of the amino acids present as NH_3^+ which interacts with the negatively charged phosphate group of the lipid bilayer. So, the electrostatic interactions also have some contribution to lipid bilayer –AuNPs interactions.

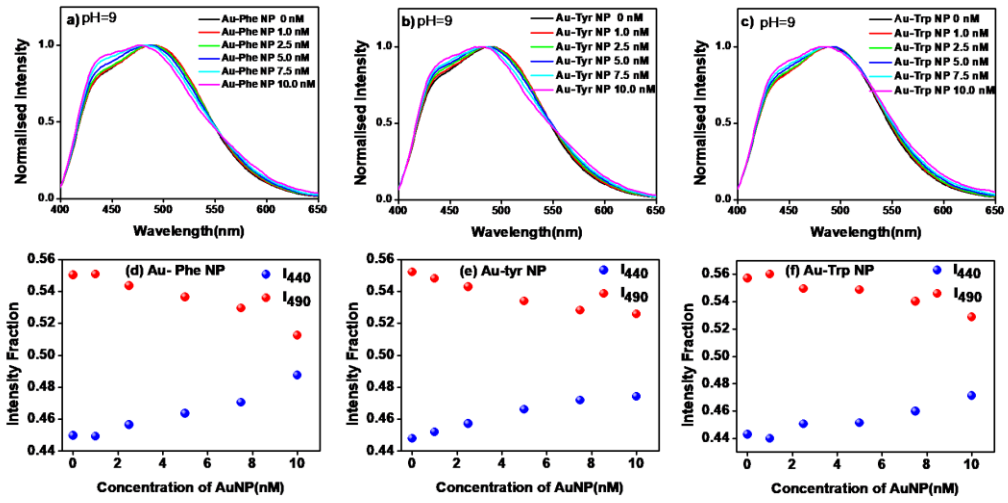

Figure 12: Steady-state normalized fluorescence spectra and corresponding area fraction plots for DMPC-PRODAN upon interaction with three AuNPs **(a-f)** at pH=9.

Now, we look into the interaction of the AuNPs with overall negative charged lipid membrane composed of DMPC: DMPG(7:3)**.** Here also Phenylalanine functionalized AuNP shows more dehydration of the lipid bilayer, followed by tyrosine functionalized AuNP, least tryptophan functionalized AuNP. **Figure 13(a-f)** shows the binding affinity of the AuNPs with the lipid bilayer. Intensity

fraction plot reveals the LE state of PRODAN and the increment of the LE state is less for tryptophan functionalized AuNP. The relative plot and Generalized Polarization data support these observations in figure **14(a-b)**.

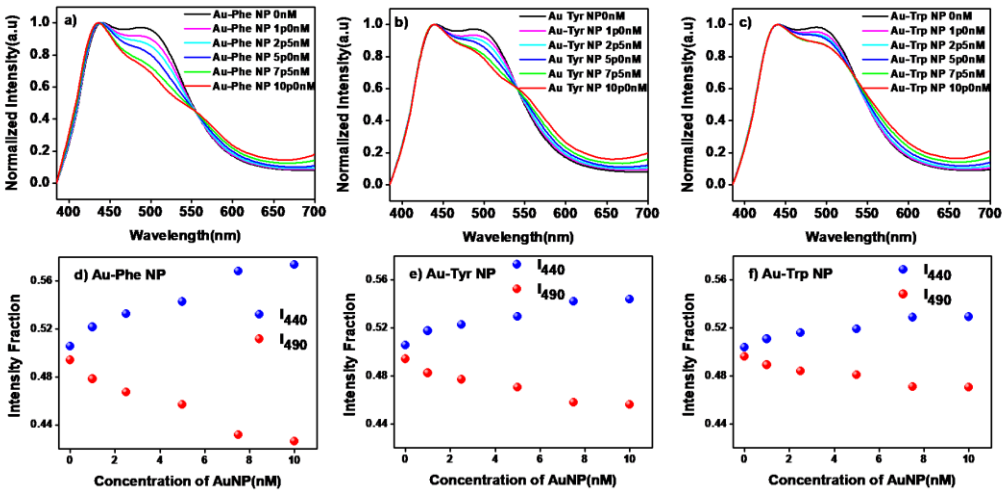

Figure 13: Steady-state normalized fluorescence spectra and corresponding area fraction plots for DMPC-DMPG-PRODAN upon interaction with three AuNPs **(a-f)** at pH=7.

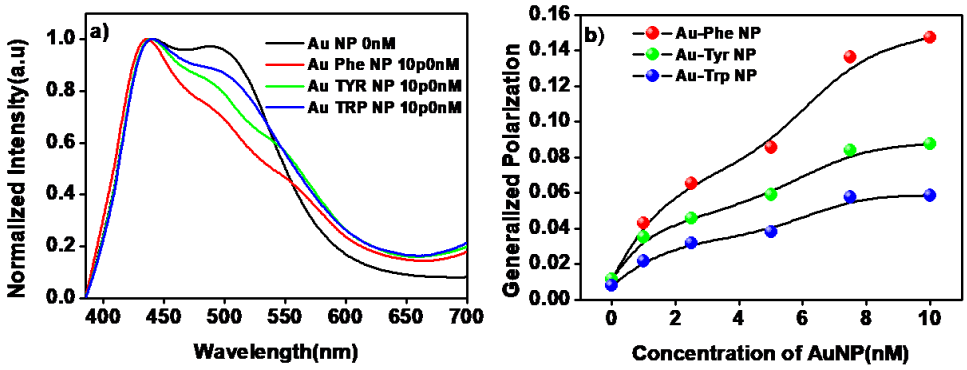

Figure 14: (a) Relative steady state normalized fluorescence spectra of DMPC-DMPG-PRODAN upon interaction with three AuNPs **(b)** Generalized Polarization data of the three AuNPs upon interaction with DMPC-DMPG bilayer.

In this case, we also found the same order of interaction of the AuNPs with DMPG lipid bilayer as like DMPC lipid bilayer. Interestingly, the interaction of

these AuNPs with the negatively charged lipid membrane is found to be a greater extent than the zwitterionic lipid membrane. We mentioned previously that Van der Waal's force is responsible for the interaction irrespective of the surface charge of the AuNPs. Greater interaction with the negatively charged lipid bilayer leads us to conclude that the NH_3^+ group of the amino acids may interact with the negatively charged phosphate group at pH=7. So, both the Van der Waal's force and electrostatic forces are responsible for greater interaction of amino acid functionalized gold nanoparticles with the negatively charged lipid bilayer. We also look into the possible aggregation of AuNPs with the DMPC:DMPG lipid bilayer. For this purpose, we take the UV-Visible spectrum of AuNPs before and after incubation. **Figure 15(a-c)** suggests that there is a negligible peak shift of the SPR band after incubation of the AuNPs.

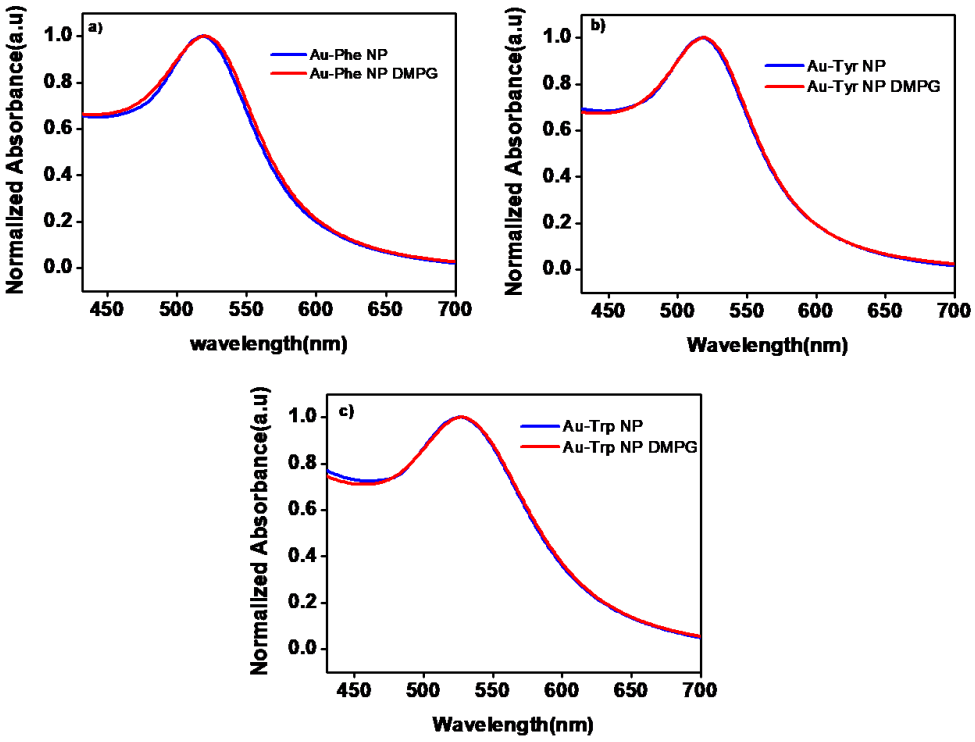

Figure 15: UV-Visible absorption spectra of AuNPs before and after incubation in DMPC-DMPG **(a-c)**.

Now as the interaction between amino acid functionalized AuNPs was investigated with the zwitterionic and negatively charged lipid bilayer, it is very

important to do the same with the positively charged lipid bilayer to get a complete view of the nature of interactions. Therefore, we conduct the experiments with positively charged lipid membrane composed of DMPC: DOTAP(7:3) at pH=7. Interestingly, from **Figure 16(a-f)** we found significant changes which indicate the interaction of the AuNPs with a positively charged lipid membrane.

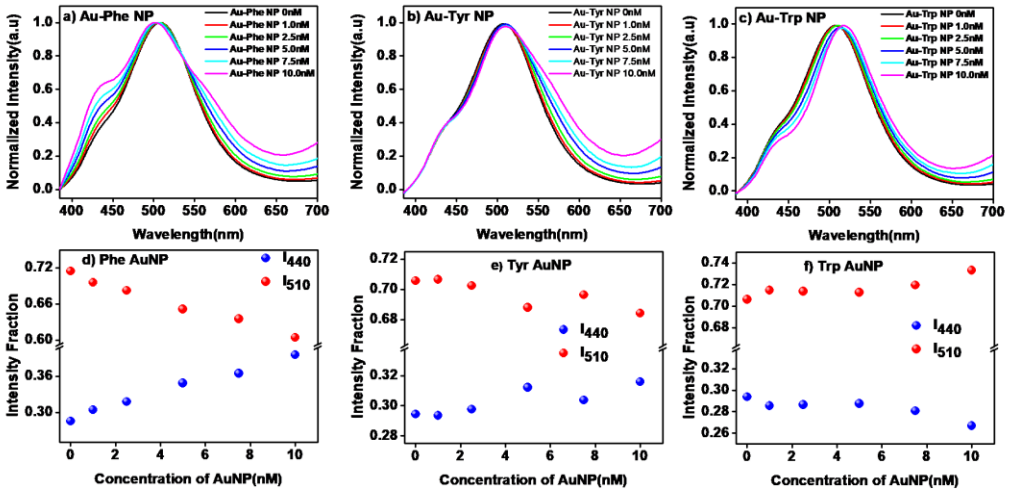

Figure 16: Steady-state normalized fluorescence spectra and corresponding area fraction plots for DMPC-DOTAP-PRODAN upon interaction with three AuNPs **(a-f)** at pH=7.

Contradictory to our previous observation, this data reveals that tryptophan functionalized AuNP induce hydration to the lipid bilayer whereas tyrosine functionalized AuNP remains unchanged and phenylalanine functionalized AuNP induces dehydration of the lipid membrane which is in accordance with our previous results. Incubation of the AuNPs into liposomes, the ruby red color of the tryptophan functionalized AuNP turns into colorless whereas the ruby red color of the tyrosine and phenylalanine functionalized AuNPs remain unchanged. **Figure 17(a-c)** is the UV data, before and after incubation of the AuNPs into DMPC: DOTAP lipid which shows the broadening of the SPR band with a significant peak shift in case of tryptophan functionalized AuNP whereas in case of phenylalanine and tyrosine functionalized AuNP there is a marginal peak shift. This data suggests that tryptophan functionalized AuNP undergo aggregation upon interaction with a positively charged lipid.

Our result suggests that the aggregation of the tryptophan functionalized AuNP may be responsible for the fluidization of the lipid membrane. It is reported that the larger size of the nanoparticles has the ability to fluidized the lipid bilayer compare to the smaller one. Our result also in accordance with the previous reports. The difference in the aggregation behavior in the presence of positively charged lipid may be due to the difference in the surface charge of the AuNPs. The Tryptophan functionalized AuNPs have zeta potential -8 mV. So with incubation of the tryptophan functionalized AuNP into liposomes the surface charges are possibly neutralized and undergo aggregation y changing the ruby red color of the AuNP. **Figure 17(a-c)** is the UV data before and after incubation of the AuNPs into DMPC: DOTAP lipid, also supports our result. But in the case of Phenylalanine functionalized AuNP the surface charge is -35 that prevents the neutralization of surface charge. So Van der Waal's force dominates over charge neutralization, causing gelation of the lipid membrane.

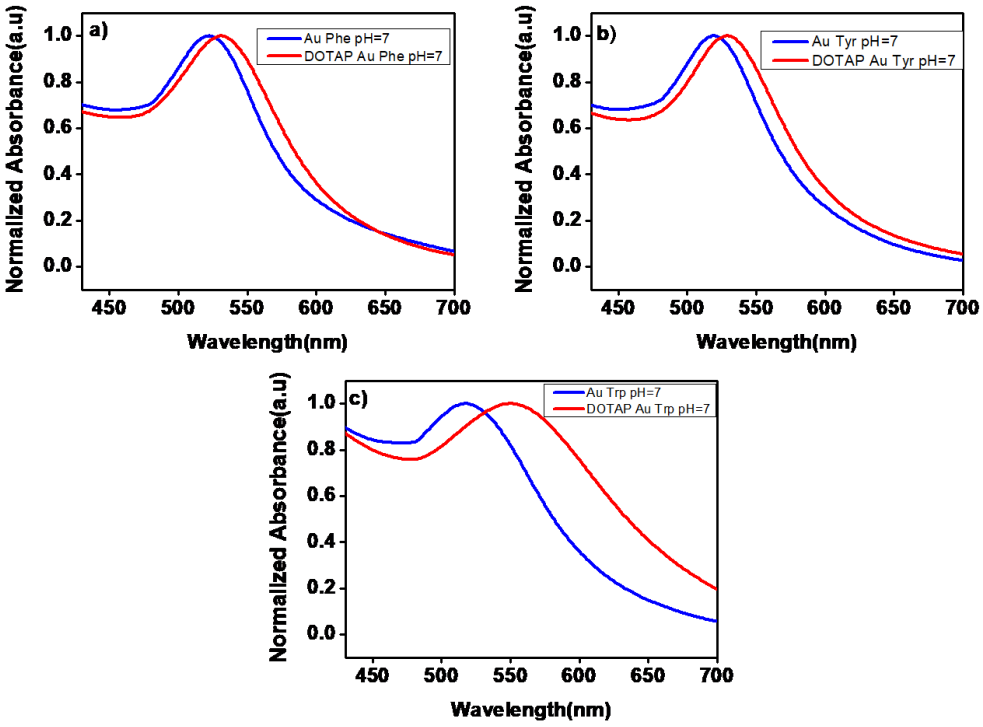

Figure 17: UV-Visible absorption spectra of AuNPs before and after incubation in DMPC-DOTAP **(a-c).**

Conclusion

In summary, we synthesized different amino acid functionalized gold nanoparticles and studied the interaction of these nanoparticles with zwitterionic, negatively and positively charged lipid bilayer. From the above studies, we summarized the following important observations:

(1) The concentration of Au^{3+}, amino acid and NaOH pay a significant role in the formation of AuNPs and the size of the AuNPs. Size of the nanoparticle can be easily tuned by the varying the concentration of amino acids.

(2) All the aromatic amino acid functionalized AuNPs showed the excitation wavelength-dependent photoluminescence properties. Among these nanoparticles, tyrosine functionalized gold nanoparticles are highly fluorescent than the other two.

(3) The bulkiness of the surface ligands is a crucial factor in the extent of gelation of the lipid membranes and the minimum gelation is observed when the ligand is bulky.

(4) Although the interaction of the nanoparticle- zwitterionic lipid bilayer is mainly driven by the van der Waals forces, electrostatic interaction between the $–NH_3^+$ and $–PO_4^{3-}$ also has an important role in case of nanoparticle-negatively charged lipid bilayer interaction.

REFERENCES

[1] Daniel M. C., Autruc D. (2004), Gold nanoparticles: assembly, supramolecular chemistry, quantum-size-related properties, and applications toward biology, catalysis, and nanotechnology. *Chem. Rev*, **104**, 293–346.

[2] Wilcoxon J P., Martin J E., Parsapour F., Wiedenman B ., Kelley D F. (1998), Photoluminescence from nanosize gold clusters. J. Chem. Phys, **108**, 9137–43.

[3] Haruta M. (2002), Catalysis of gold nanoparticles deposited on metal oxides. *Cattech,* **6**, 102–15.

[4] Link S., El-Sayed M A. (2003) Optical properties and ultrafast dynamics of metallic nanocrystals Annu. *Rev. Phys. Chem*, **54**, 331–66.

[5] Link S., El-Sayed M A. (1999) Spectral properties and relaxation dynamics of surface plasmon electronic oscillations in gold and silver nanodots and nanorods. *J. Phys. Chem. B*, **103**, 8410–26.

[6] Link S., El-SayedM A. (1999) Size and temperature dependence of the plasmon absorption of colloidal gold nanoparticles. *J. Phys. Chem. B*, **103**, 4212–7.

[7] Sardar R., Funston A. M., Mulvaney P., Murray R. W. (2009), Gold nanoparticles: past, present, and future. *Langmuir,* **25**, 13840–13851.

[8] Ghodake G., Rasool K., Seo Y. G., Lim S. R., Lee D. S. (2013), Green Synthesis of Gold Nanoparticles by Amino Acids: Bioconjugation and UV-Fluorescence, *J. Nanoelectron. Optoelectron*, **8**, 535-539.

[9] Giljohann D. A., Seferos D. S., Daniel W. L., Massich M. D., Patel P. C., Mirkin C. A. (2010), Gold nanoparticles for biology and medicine, *Angew. Chem., Int. Ed*. **49**, 3280–3294.

[10] Homberger M., Simon U. (2010), On the application potential of gold nanoparticles in nanoelectronics and biomedicine, Philos. *Trans. R. Soc. A*, **368**, 1405–1453.

[11] Sperling R. A., Gil P. R., Zhang F., Zanella M., Parak W. J. (2008), Biological applications of gold nanoparticles. *Chem. Soc. Rev*, **37**, 1896–1908.

[12] Jain P. K., El-Sayed I. H., El-Sayed M. A. (2007), Au nanoparticles target cancer. *Nanotoday*, **2**, 18–29.

[13] Shan J., Tenhu H. (2007), Recent advances in polymer protected gold nanoparticles: synthesis, properties and applications. *Chem. Commun*, **44**, 4580-4598.

[14] Bajpai S. K., Mohan Y. M., Bajpai M., Tankhiwale R., Thomas, V. (2007), Synthesis of polymer stabilized silver and gold nanostructures. *J. Nanosci. Nanotechnol*, **7**, 2994-3010.

[15] Goy-López S., Castro E., Taboada P., Mosquera V. (2008), Block copolymer-mediated synthesis of size-tunable gold nanospheres and nanoplates. *Langmuir*, **24**, 13186-13196.

[16] Sau T. K., Murphy, C. J. (2004), Room temperature, high-yield synthesis of multiple shapes of gold nanoparticles in aqueous solution. *J. Am. Chem. Soc*, **126**, 8648-8649.

[17] Piella J., Bastús N. G., Puntes V. (2016), Size-Controlled Synthesis of Sub-10-nanometer Citrate-Stabilized Gold Nanoparticles and Related Optical Properties. *Chem. Mater*, **28**, 1066-1075.

[18] Ji X., Song X., Li J., Bai Y., Yang W., Peng X. (2007), Size control of gold nanocrystals in citrate reduction: the third role of citrate. *J. Am. Chem. Soc*, **129**, 13939-13948.

[19] Si S., Bhattacharjee R. R., Banerjee A., Mandal T. K. (2006), A Mechanistic and Kinetic Study of the Formation of Metal Nanoparticles by Using Synthetic Tyrosine-Based Oligopeptides. *Chem.: Eur. J*, **12**, 1256-1265.

[20] Sakai T., Alexandridis P. (2005), Size-and shape-controlled synthesis of colloidal gold through autoreduction of the auric cation by poly (ethylene oxide)–poly (propylene oxide) block copolymers in aqueous solutions at ambient conditions. *Nanotechnology*, **16**, S344.

[21] Sakai T., Alexandridis P. (2006), Ag and Au monometallic and bimetallic colloids: morphogenesis in amphiphilic block copolymer solutions. *Chem. Mater*, **18**, 2577-2583.

[22] Rahme K., Oberdisse J., Schweins R., Gaillard C., Marty J. D., Mingotaud C., Gauffre, F. (2008), Pluronics-Stabilized Gold Nanoparticles: Investigation of the Structure of the Polymer–Particle Hybrid. *ChemPhysChem*, **9**, 2230-2236.

[23] Bakshi M. S., Kaura A., Bhandari P., Kaur G., Torigoe K., Esumi K. (2006), Synthesis of colloidal gold nanoparticles of different morphologies in the presence of triblock polymer micelles. *J. Nanosci. Nanotechnol*, **6**, 1405-1410.

[24] Gao J., Huang X., Liu H., Zan F., Ren J. (2012), Colloidal stability of gold nanoparticles modified with thiol compounds: bioconjugation and application in cancer cell imaging. *Langmuir*, **28**, 4464-4471.

[25] Zhao J., Wu Y., Tao H., Chen H., Yang W., Qiu S. (2017), Colorimetric detection of streptomycin in milk based on peroxidase-mimicking catalytic activity of gold nanoparticles. *RSC Advances*, **7**, 38471-38478.

[26] Magura J., Zeleňáková A., Zeleňák V., Kaňuchová M. (2014), Thiol-modified gold nanoparticles deposited on silica support using dip coating. *Appl. Surf. Sci*, **315**, 392-399.

[27] Gole A., Dash C., Ramakrishnan V., Sainkar S. R., Mandale A. B., Rao M., Sastry M. (2001), Pepsin− gold colloid conjugates: preparation, characterization, and enzymatic activity. *Langmuir*, **17**, 1674-1679.

[28] Bhattacharjee R. R., Chakraborty M., Mandal T. K. (2006), Reversible association of thermoresponsive gold nanoparticles: polyelectrolyte effect on the lower critical solution temperature of poly (vinyl methyl ether). *J. Phys. Chem. B*, **110**, 6768-6775.

[29] Hayat M. A. (2012), Colloidal gold: principles, methods, and applications. *Elsevier*.

[30] Aslam M., Fu L., Su M., Vijayamohanan K., Dravid V. P. (2004), Novel one-step synthesis of amine-stabilized aqueous colloidal gold nanoparticles. *J. Mater. Chem*, **14**, 1795-1797.

[31] Selvakannan P. R., Mandal S., Phadtare S., Gole A., Pasricha R., Adyanthaya S. D., Sastry M. (2004), Water-dispersible tryptophan-protected gold nanoparticles prepared by the spontaneous reduction of aqueous chloroaurate ions by the amino acid. *J. Colloid Interface Sci*, **269**, 97-102.

[32] Prince R. C. (1988), Tyrosine radicals. *Trends in biochemical sciences*, **13**, 286-288.

[33] Hoffman B. M., Roberts J. E., Kang C. H., Margoliash E. (1981), Electron paramagnetic and electron nuclear double resonance of the hydrogen peroxide compound of cytochrome c peroxidase. *J. Biol. Chem*, **256**, 6556-6564.

[34] Sivaraja M., Goodin D. B., Smith M., Hoffman B. M. (1989), Identification by ENDOR of Trp191 as the free-radical site in cytochrome c peroxidase compound. *ES. Science*, **245**, 738-740.

[35] Covès J., Delon B., Climent I., Sjöberg B. M., Fontecave M. (1995), Enzymic and Chemical Reduction of the Iron Center of the Escherichia coli

Ribonucleotide Reductase Protein R2: The Role of the C-Terminus. *Eur J Biochem*, **233**, 357-363.

[36] Lendzian F., Sahlin M., MacMillan F., Bittl R., Fiege R., Pötsch S., Lassmann, G. (1996), Electronic structure of neutral tryptophan radicals in ribonucleotide reductase studied by EPR and ENDOR spectroscopy. *J. Am. Chem. Soc*, **118**, 8111-8120.

[37] Essenmacher C., Kim S. T., Atamian M., Babcock G. T., Sancar, A. (1993), Tryptophan radical formation in DNA photolyase: electron-spin polarization arising from photoexcitation of a doublet ground state. *J. Am. Chem. Soc*, **115**, 1602-1603.

[38] Heelis P. F., Okamura T., Sancar A. (1990), Excited-state properties of Escherichia coli DNA photolyase in the picosecond to millisecond time scale. *Biochemistry*, **29**, 5694-5698.

[39] Si S., Mandal, T. K. (2007), Tryptophan-based peptides to synthesize gold and silver nanoparticles: A mechanistic and kinetic study. *Chem.: Eur. J*, **13**, 3160-3168.

[40] Tsukada, et al (2015), Spectroscopic and Morphological Studies on Interaction between Gold Nanoparticle and Liposome Constructed with Phosphatidylcholine. *IOP CONF. SER. MATER. SCI*, **76**, 012001

[41] Kanwa N., De S. K., Adhikari C., Chakraborty A. (2017), Spectroscopic Study of the Interaction of Carboxyl-Modified Gold Nanoparticles with Liposomes of Different Chain Lengths and Controlled Drug Release by Layer-by-Layer Technology. *J. Phys. Chem. B*, **121**, 11333-11343.

[42] www.bioexplorer.net

[43] Thamphiwatana S., Fu V., Zhu J., Lu D., Gao W., Zhang L. (2013), Nanoparticle-stabilized liposomes for pH-responsive gastric drug delivery. *Langmuir*, **29**, 12228-12233.

[44] Adhikari C., Das A., Chakraborty A. (2015), Controlled Release of a Sparingly Water-Soluble Anticancer Drug through pH-Responsive Functionalized Gold-Nanoparticle-Decorated Liposomes, *ChemPhysChem*, **16**, 866-871.

[45] Pornpattananangkul D., Olson S., Aryal S., Sartor M., Huang C. M., Vecchio K., Zhang, L. (2010), Stimuli-responsive liposome fusion mediated by gold nanoparticles. *ACS nano*, **4**, 1935-1942.

[46] Yu Y., Anthony S. M., Zhang L., Bae S. C., Granick S. (2007), Cationic nanoparticles stabilize zwitterionic liposomes better than anionic ones. *J. Phys. Chem. C*, **111**, 8233-8236.

[47] De S. K., Kanwa N., Ahamed M., Chakraborty A. (2018), Spectroscopic evidence for hydration and dehydration of lipid bilayers upon interaction with metal ions: a new physical insight. *Phys. Chem. Chem. Phys*, **20**, 14796-14807.

[48] Binder H., Zschörnig O. (2002), The effect of metal cations on the phase behavior and hydration characteristics of phospholipid membranes. *Chemistry and physics of lipids*, **115**, 39-61.

[49] Hong H., Tamm L. K. (2004), Elastic coupling of integral membrane protein stability to lipid bilayer forces, Proceedings of the National Academy of Sciences. **101**, 4065-4070.

[50] Vafaei S., Tabaei S. R., Cho N. J. (2017), Optimizing the performance of supported lipid bilayers as cell culture platforms based on extracellular matrix functionalization. *ACS omega*, **2**, 2395-2404.

[51] Bangham A. D., De Gier J., Greville G. D. (1967), Osmotic properties and water permeability of phospholipid liquid crystals. *Chemistry and physics of lipids*, **1**, 225-246.

[52] Szoka F., Papahadjopoulos D. (1978), Procedure for preparation of liposomes with large internal aqueous space and high capture by reverse-phase evaporation. *Proceedings of the national academy of sciences*, **75**, 4194-4198.

[53] Deamer D., Bangham A. D. (1976), Large volume liposomes by an ether vaporization method. *Biochimica et Biophysica Acta (BBA)-Nucleic Acids and Protein Synthesis*, **443**, 629-634.

[54] Al-Jamal W. T., Kostarelos K. (2007), Liposome–nanoparticle hybrids for multimodal diagnostic and therapeutic applications. *Nanomedicine*, **2**, 85-98

[55] Preiss M. R., Bothun G. D. (2011), Stimuli-responsive liposome-nanoparticle assemblies. *Expert opinion on drug delivery*, **8**, 1025-1040.

[56] Paasonen, et al (2010), Gold-Embedded Photosensitive Liposomes for Drug Delivery: Triggering Mechanism and Intracellular Release. *J. Control. Release*, **147**,136-143.

[57] Liu J., Jiang X., Ashley C., Brinker C. J. (2009), Electrostatically mediated liposome fusion and lipid exchange with a nanoparticle-supported bilayer for control of surface charge, drug containment, and delivery. *J. Am. Chem. Soc*, **131**, 7567-7569.

[58] Tan S., Li X., Guo Y., Zhang Z. (2013), Lipid-enveloped hybrid nanoparticles for drug delivery. *Nanoscale*, **5**, 860-872.

[59] Abraham S., Narine S. S. (2011), A facile synthesis of lipid stabilized gold nanoparticles: a step towards biodegradable biosensors. *J. Nanosci. Nanotechnol*, **11**, 7027-7032.

[60] Mornet S., Lambert O., Duguet E., Brisson, A. (2005), The formation of supported lipid bilayers on silica nanoparticles revealed by cryoelectron microscopy. *Nano letters*, **5**, 281-285.

[61] Gao W., Hu C. M. J., Fang R. H., Zhang L. (2013), Liposome-like nanostructures for drug delivery. *J. Mater. Chem. B*, **1**, 6569-6585.

[62] Tan S., Li X., Guo Y., Zhang Z. (2013), Lipid-enveloped hybrid nanoparticles for drug delivery. *Nanoscale*, **5**, 860-872.

[63] Liu Y., Wang F., Liu J. (2018), Headgroup-Inversed Liposomes: Biointerfaces, Supported Bilayers and Applications. *Langmuir*, **34**, 9337-9348.

[64] Wang F., and Liu J., (2014), Liposome supported metal oxide nanoparticles: interaction mechanism, light controlled content release, and intracellular delivery. *Small*, **10**, 3927–31.

[65] Liu Y., Liu J. (2017), Zn2+ Induced Irreversible Aggregation, Stacking, and Leakage of Choline Phosphate Liposomes. *Langmuir*, **33**, 14472-14479.

[66] Reimhult E., Höök F., Kasemo B. (2003), Intact vesicle adsorption and supported biomembrane formation from vesicles in solution: influence of surface chemistry, vesicle size, temperature, and osmotic pressure. *Langmuir*, **19**, 1681-1691.

[67] Mustafa D. E., Yang T., Xuan Z., Chen S., Tu H., Zhang A. (2010), Surface plasmon coupling effect of gold nanoparticles with different shape and size on conventional surface plasmon resonance signal. *Plasmonics*, **5**, 221-231.

[68] Wang X., Gogol P., Cambril E., Palpant B. (2012), Near-and far-field effects on the plasmon coupling in gold nanoparticle arrays. *J. Phys. Chem. C*, **116**, 24741-24747.

[69] Zhang L., Granick S. (2006), How to stabilize phospholipid liposomes (using nanoparticles). *Nano letters*, **6**, 694-698.

[70] Mohapatra M., Mishra A. K. (2013), Photophysical Behavior of 8-Anilino-1-Naphthalenesulfonate in Vesicles of Pulmonary Surfactant Dipalmitoylphosphatidylcholine (DPPC) and Its Sensitivity toward the Bile Salt–Vesicle Interaction. *Langmuir*, **29**, 11396-11404.

[71] Parasassi T., Krasnowska E. K., Bagatolli L., Gratton E. (1998), Laurdan and Prodan as polarity-sensitive fluorescent membrane probes. *journal of fluorescence*, **8**, 365-373.

[72] Krasnowska E. K., Gratton E., Parasassi T. (1998), Prodan as a membrane

surface fluorescence probe: partitioning between water and phospholipid phases. *Biophysical journal*, **74**, 1984-1993.

[73] Wilson-Ashworth H. A., Bahm Q., Erickson J., Shinkle A., Vu M. P., Woodbury D., Bell, J. D. (2006), Differential detection of phospholipid fluidity, order, and spacing by fluorescence spectroscopy of bis-pyrene, prodan, nystatin, and merocyanine 540. *Biophysical journal*, **91**, 4091-4101.

[74] Novaira M., Biasutti M. A., Silber J. J., Correa N. M. (2007), New insights on the photophysical behavior of PRODAN in anionic and cationic reverse micelles: from which state or states does it emit?. *J. Phys. Chem. B*, **111**, 748-759.

[75] Gutowicz J., Krawczyk A. (1986), Effects of 1-anilinonaphthalene-8-sulphonate on phase transition temperature of dipalmitoylphosphatidylcholine liposomes. *Chemistry and physics of lipids*, **39**, 357-364.

[76] Lesslauer W., Cain J. E., Blasie J. K. (1972), X-ray diffraction studies of lecithin bimolecular leaflets with incorporated fluorescent probes. *Proceedings of the National Academy of Sciences*, **69**, 1499-1503.

[77] Lesslauer W., Cain J., Blasie, J. K. (1971), On the location of 1-anilino-8-naphthalene-sulfonate in lipid model systems: An X-ray diffraction study. *Biochimica et Biophysica Acta (BBA)-Biomembranes*, **241**, 547-566.

[78] Gulik-Krzywicki T., Shechter E., Iwatsubo M., Ranck J. L., Luzzati V. (1970), Correlations between structure and spectroscopic properties in membrane model systems trytophan and i-anilino-8-naphtalene sulfonate fluorescence in protein-lipid-water phases. *Biochimica et Biophysica Acta (BBA)-Biomembranes*, **219**, 1-10.

[79] Kosower E. M., Kanety H. (1983), Intramolecular donor-acceptor systems. 10. Multiple fluorescences from 8-(N-phenylamino)-1-naphthalenesulfonates. *J. Am. Chem. Soc*, **105**, 6236-6243.

[80] Kim D. Y., Kim M., Shinde S., Saratale R. G., Sung J. S., Ghodake G. (2017), Temperature Dependent Synthesis of Tryptophan-Functionalized Gold Nanoparticles and Their Application in Imaging Human Neuronal Cells. *ACS Sustain. Chem. Eng*, **5**, 7678-7689.

[81] Kim D. Y., Shinde S., Saratale R., Syed A., Ameen F., Ghodake G. (2017),

Spectrophotometric determination of Fe (III) by using casein-functionalized gold nanoparticles. *Microchimica Acta*, **184**, 4695-4704.

[82] Shinde S., Kim D. Y., Saratale R., Syed A., Ameen F., Ghodake, G. (2017), A Spectral Probe for Detection of Aluminum (III) Ions Using Surface Functionalized Gold Nanoparticles. *Nanomaterials*, **7,** 287.